THE

PHYSICAL REVIEW

A journal of experimental and theoretical physics established by E. L. Nichols in 1893

SECOND SERIES, VOL. 72, No. 9 NOVEMBER, 1 1947

High Energy Photo-Disintegration of the Deuteron*

M. E. ROSE AND G. GOERTZEL
Clinton Laboratories, Oak Ridge, Tennessee

(Received June 30, 1947)

The disintegration of the deuteron by γ-rays in the range 50-250 Mev is investigated. The lower energy limit is imposed by the neglect of nuclear forces between the neutron and proton after absorption of the photon. Moreover, the effects of retardation and of multipole radiation higher than dipole, the investigation of which constitutes one of the primary purposes of the present work, become apparent only above 50 Mev. The upper limit is imposed by the assumption that the nuclear particles can be treated non-relativistically. It is shown that at the high radiation energies considered it is essential to take into account the range of the nuclear forces in the ground state and that this is the case because of the importance of interference effects (short de Broglie wave-length of the nucleons) which depend very strongly on the "size" of the deuteron. The cross section at 50 Mev is $37\mu b(37\times 10^{-30}\text{ cm}^2)$ and decreases with γ-ray energy up to 150 Mev as $(\hbar\omega)^{-n}$ where n lies between 4 and 5. Beyond 150 Mev the cross section decreases less rapidly because of a more favorable phase relation between outgoing waves from different parts of the deuteron. The general features of the cross section and of the angular distribution of the particles can be understood in terms of interference; the most important effect of the interference is to favor strongly small momentum for the recoil particle (proton in the case of charge coupling and both proton and neutron in the case of spin coupling). The error caused by neglect of nuclear forces in the final state is estimated, by a consideration of electric dipole transitions, to be less than 30 percent in the worst case (low energy photons). The effects of retardation and higher multipoles are calculated explicitly, and it is shown that these effects are small at 50 Mev and important at 100 Mev. It is also shown that the effect of non-central forces between the nucleons in the ground state introduces negligible error.

I. INTRODUCTION

WITH the availability of high energy radiation from the betatron and synchrotron the question of the photo-disintegration of nuclei becomes an interesting one. In general terms the primary problem is to obtain an understanding of the behavior of a nuclear system in the high energy region where the pertinent de Broglie wave-lengths are comparable with the size of the system and, eventually, with the range of the nuclear forces. From the theoretical point of view the case of greatest interest is the dissociation of the deuteron, not only because of the comparative simplicity of this system, but also because only in this case may one expect the photo-particles to be very energetic.

It is therefore our purpose to obtain reasonably reliable values for the photo-disintegration cross section for γ-rays of energies above 50 Mev, where the strong interference effects of high energies begin to appear. Previous investigations[1] which are applicable at low energies involve the neglect of retardation and the neglect of multi-

* This document is based on work performed under Contract No. W-35-058-eng-71 for the Manhattan Project at the Clinton Laboratories.

[1] H. A. Bethe and R. Peierls, Proc. Roy. Soc. **A148**, 146 (1935); E. U. Condon and G. Breit, Phys. Rev. **49**, 904 (1936); H. A. Bethe, Rev. Mod. Phys. **8**, 82 (1936); K. Way, Phys. Rev. **51**, 552 (1937); A Pais, Det. Kgl. Danske Videns. Selskab. Mat.-Fys. Medd. Bind **20**, No. 17 (1943).

poles higher than electric and magnetic dipole.[2] As will be shown below, the retardation and higher multipoles may be neglected for γ-ray energies up to about 50 Mev. For more energetic radiation these effects become significant and must be taken into account. Of even greater importance is the finite range of the nuclear forces. It has already been shown that the finite range has an appreciable effect on the cross section at low energies.[1] At high energies, where the wave-length of the nucleons after absorption of the photon is small, a proper representation of the effects of interference is obtained only by a correct representation of the size of the deuteron, which requires consideration of the finite range of the forces.[3]

An additional motive for investigation of the high energy photo-disintegration might be found in the possibility of obtaining information about nuclear forces in P states or in states of even higher angular momentum. However, because of the small cross sections involved, if for no other reason, the photo-process does not seem eminently suitable for this purpose. In view of the present information about nuclear forces it seemed most appropriate to limit the following considerations to energies such that the effect of the interaction between neutron and proton could be neglected in the final state. For this reason the following calculations were restricted to γ-energies$\geqslant 50$ Mev. An upper limit of 250-Mev photons was imposed by the neglect of relativistic effects.

II. CALCULATION OF THE CROSS SECTION

The differential cross section for the photo-disintegration by a γ-ray of energy $\hbar\omega$, in which the relative motion of the nucleons in the zero-momentum reference frame[4] lies in the solid angle $d\Omega$ is

$$d\sigma = (d\Omega/4\pi)(e^2/\hbar c)(hk/M\omega)(|W|^2)_{\mathrm{Av}}. \quad (1)$$

[2] The effect of the electric quadripole part of the incident radiation at 17.5 Mev was calculated by W. Rarita and J. Schwinger, Phys. Rev. **59**, 556 (1941) and, as expected, the corresponding cross section is small.

[3] The cross section for the photo-disintegration at high energies as calculated by J. M. Jauch, Phys. Rev. **69**, 275 (1946) is much too large because of the neglect of the interference arising from the finite range.

[4] That is, the frame in which the total momentum of the system of deuteron plus photon is zero. Thus, before the absorption the deuteron travels in a direction opposite to the photon with energy $E_c = (\hbar\omega)^2/4Mc^2$.

In (1) the symbol Av means an average over the polarization directions of the radiations, over the magnetic substates of the initial state, and a sum over the magnetic substates of the final state. W is the matrix element

$$W = (\Psi_f, w\Psi_i) \quad (2)$$

where the ground state wave function Ψ_i is normalized to unity and the final state wave function is defined so that its asymptotic behavior is a unit amplitude plane wave with the relative momentum $\hbar\mathbf{k}$ plus a converging spherical wave. Where the particles are regarded as free in the final state the spherical wave vanishes and Ψ_f is exactly equal to the unit amplitude plane wave.

In (2) $(e\hbar/Mc)w$ is the perturbation caused by the interaction of the radiation with the charge of the proton and the spins of the two nucleons. We write the vector potential of the radiation as

$$\mathbf{A}(\boldsymbol{\rho}) = \boldsymbol{\pi} \exp[i(\mathbf{k}_0\cdot\boldsymbol{\rho} - \omega t)] + \boldsymbol{\pi}^* \exp[-i(\mathbf{k}_0\cdot\boldsymbol{\rho} - \omega t)], \quad (3)$$

where $\boldsymbol{\pi}$ is a unit polarization vector. Then

$$w = i \exp[i\mathbf{k}_0\cdot\mathbf{r}/2]\boldsymbol{\pi}\cdot\mathrm{grad} - \tfrac{1}{2}[\mu_p\boldsymbol{\sigma}_p\cdot\mathbf{H}(\tfrac{1}{2}\mathbf{r}) + \mu_n\boldsymbol{\sigma}_n\cdot\mathbf{H}(-\tfrac{1}{2}\mathbf{r})], \quad (4)$$

where $\mathbf{H}$ is the magnetic field derivable from (3), μ_n and μ_p are the magnetic moments of neutron and proton, respectively, in units $e\hbar/2Mc$, and $\mathbf{r} = \mathbf{r}_p - \mathbf{r}_n$ is the vector separation of the particles. The $\boldsymbol{\sigma}_n$ and $\boldsymbol{\sigma}_p$ are the Pauli spin-vectors.

The center of gravity motion has been separated out, giving conservation of total linear momentum as usual, so that the relative coordinates of the particles with respect to the centroid appear as argument in $\mathbf{H}$. Thus (4) has been written in accordance with the fact that because of retardation there is a phase difference in the outgoing waves caused by the spins of the two nucleons.

The first term of (4) gives rise to what will be called the charge transitions, while the remaining terms give the so-called spin transitions.[5] The

[5] The more customary terminology (photoelectric and photo-magnetic transitions, respectively) seems somewhat ambiguous for the present discussion where the incident

spin operator in (4) can be split into two parts, one symmetric and the other antisymmetric in the spins of the particles. Therefore, while the charge transitions always lead from a triplet ground state to a triplet final state, the spin transitions lead to both triplet and singlet final states. In contrast to the situation at low energies, the former type of spin transition does not vanish. This is due to the retardation and, incidentally, to the neglect of the forces in the final state. Designating the matrix element for the charge transition by W_c and those for the triplet-triplet and triplet-singlet spin transitions by W_{s1} and W_{s0}, respectively, we find

$$(|W|^2)_{\text{Av}}=(|W_c|^2)_{\text{Av}}+(|W_{s1}|^2)_{\text{Av}}+(|W_{s0}|^2)_{\text{Av}}. \quad (5)$$

Because the spin transitions involve a change in spin orientation ($\Delta m_s\neq 0$) the charge and spin transitions do not interfere. The two types of spin transition, while non-cohering, are each composed of cohering contributions from the neutron and proton spins.

In the following we shall neglect non-central forces between the nuclear particles in the ground state.[6] Then the total spin is a good quantum number and

$$\Psi_f=\psi_f\chi_{0,\,1}{}^{m_s} \quad (6)$$

where ψ_f depends on spatial coordinates only and $\chi_{0,\,1}{}^{m_s}$ is a spin function for singlet and triplet states, respectively. For the ground state

$$\Psi_i=\psi_i\chi_1{}^{m_s'}, \quad (6a)$$

Then

$$W_c=i\boldsymbol{\pi}\cdot(\psi_f,\ \exp[i\tfrac{1}{2}\mathbf{k}_0\cdot\mathbf{r}]\ \text{grad}\psi_i)\delta_{m_sm_s'}, \quad (7a)$$

$$W_{si}=-\frac{i}{2}(\mathbf{k}_0\times\boldsymbol{\pi})\cdot\mathbf{u}_{m_sm_s'}[\mu_p(\psi_f,\ \exp[i\tfrac{1}{2}\mathbf{k}_0\cdot\mathbf{r}]\psi_i)$$
$$+\mu_n(\psi_f,\ \exp[-i\tfrac{1}{2}\mathbf{k}_0\cdot\mathbf{r}]\psi_i)], \quad (7b)$$

$$W_{s0}=-\frac{i}{2}(\mathbf{k}_0\times\boldsymbol{\pi})\cdot\mathbf{v}_{m_sm_s'}[\mu_p(\psi_f,\ \exp[i\tfrac{1}{2}\mathbf{k}_0\mathbf{r}]\psi_i)$$
$$-\mu_n(\psi_f,\ \exp[-i\tfrac{1}{2}\mathbf{k}_0\cdot\mathbf{r}]\psi_i)], \quad (7c)$$

where

$$\mathbf{u}_{m_sm_s'}=(\chi_1{}^{m_s},\ \boldsymbol{\sigma}_p\chi_1{}^{m_s'}), \quad (7d)$$

$$\mathbf{v}_{m_sm_s'}=(\chi_0{}^0,\ \boldsymbol{\sigma}_p\chi_1{}^{m_s'}). \quad (7e)$$

(1) Calculation of the Matrix Elements

For no nuclear forces between particles in the final state, we have simply

$$\psi_f=\exp i(\mathbf{k}\cdot\mathbf{r}), \quad (6a)$$

where the wave vector $\mathbf{k}$ is in the direction of proton momentum in the zero-momentum reference frame. From (7) we obtain

$$(|W_c|^2)_{\text{Av}}=\tfrac{1}{2}k^2\sin^2\vartheta I^2(q), \quad (8a)$$

$$(|W_{s1}|^2)_{\text{Av}}=(k_0^2/12)[\mu_pI(q)+\mu_nI(q')]^2, \quad (8b)$$

$$(|W_{s0}|^2)_{\text{Av}}=(k_0^2/24)[\mu_pI(q)-\mu_nI(q')]^2, \quad (8c)$$

where ϑ is the angle between the relative motion and the direction of propagation of the photon. The matrix elements are thus seen to depend essentially on the single quantity I defined by

$$I(q)=\int\exp[i\mathbf{q}\cdot\mathbf{r}]\psi_i(r)d\tau \quad (9)$$

and

$$\mathbf{q}=\mathbf{k}-\tfrac{1}{2}\mathbf{k}_0, \quad (10a)$$

$$\mathbf{q}'=\mathbf{k}+\tfrac{1}{2}\mathbf{k}_0. \quad (10b)$$

Evidently $\hbar\mathbf{q}$ and $\hbar\mathbf{q}'$ are the momenta of the neutron and proton, respectively, in the laboratory frame. Therefore, in the case of each interaction term in the hamiltonian (cf. (4)) the transition probabilities depend on the magnitude of the momentum of the recoil particle. Obviously $q'(\vartheta)=q(\pi-\vartheta)$.

To evaluate (9) the ground state wave function for a rectangular potential hole is used. The depth of the hole is V_0 and the range is R. Then with the following notation

$$x=r/R,\quad a=\alpha R=R(M\epsilon)^{\frac{1}{2}}/\hbar,$$
$$b=R[M(V_0-\epsilon)]^{\frac{1}{2}}/\hbar, \quad (11)$$

where ϵ is the binding energy of the deuteron, the wave function ψ_i becomes

$$\left.\begin{aligned}\psi_i&=(2\pi R^3)^{-\frac{1}{2}}(a/1+a)^{\frac{1}{2}}\sin bx/x,\quad x<1,\\ \psi_i&=(2\pi R^3)^{-\frac{1}{2}}(a/1+a)^{\frac{1}{2}}\sin b\,e^{-a(x-1)}/x,\quad x>1\end{aligned}\right\} \quad (12)$$

and $b\cot b=-a$,

radiation may be decomposed into the infinite series of electric and magnetic multipoles. Both types of multipoles give rise to transitions caused by coupling with the charge and spins of the particles.

[6] The effect of tensor forces in the ground state is estimated in Section 3 of this paper and is found to be negligible.

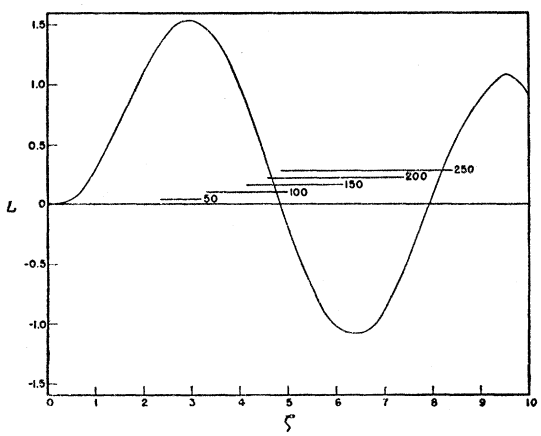

FIG. 1. The quantity L as a function of ζ, the recoil momentum in units $\hbar/R$. The horizontal segments give the range of recoil momenta, corresponding to all possible directions of the photo-particles, for gamma-ray energies (in Mev) given by the affixed numbers.

Introducing the dimensionless "recoil momentum" $\zeta = qR$, we obtain

$$I(q) = (8\pi R^3)^{\frac{1}{2}}(a/1+a)^{\frac{1}{2}}(a^2+b^2) \times \sin b(L(\zeta)/\zeta^4), \quad (13)$$

$$L(\zeta) = \zeta^4/[(a^2+\zeta^2)(b^2-\zeta^2)] \times (\cos\zeta + a\sin\zeta/\zeta). \quad (13a)$$

Because of its importance for the interpretation of the results the quantity $L(\zeta)$ is given in Fig. 1. Obviously the matrix element I decreases quite rapidly with ζ. The values of ζ corresponding to various directions for the emerging particles is given by

$$\zeta^2 = R^2(k^2 + \tfrac{1}{4}k_0{}^2 - kk_0\cos\vartheta). \quad (14)$$

The horizontal segments in Fig. 1 give the range of ζ corresponding to $0 \leqslant \vartheta \leqslant \pi$ for several γ-ray energies. It is clear that for the range of interest the approximation of zero range of the forces gives

$$I(q) = (8\pi\alpha)^{\frac{1}{2}}/(\alpha^2+q^2), \quad (R=0). \quad (13b)$$

This means that the assumption of zero range is an extremely poor one. In this approximation the oscillations in the matrix element as shown in Fig. 1, are entirely overlooked so that the destructive interference between contributions to the outgoing wave arising from different parts of the deuteron is ignored. As a result the cross section is grossly overestimated (see Section 4, below).

(2) Angular Distribution

The angular distribution of the particles in the zero-momentum reference frame $A_0(\mu)$ is obtained from (5), (8), (13), and (14). For the numerical results we have used the generally accepted value $R = 2.8\times 10^{-13}$ cm, so that $a = 0.645$ and $b = 1.898$. The results for several γ-ray energies are shown in Fig. 2. In order to facilitate the comparison between different energies all distributions are normalized to the same area.

It is of interest to compare the angular distributions obtained with that to be expected at low energies. At low energies for which only the charge transitions are important the angular distribution is $A_0 \sim 1-\mu^2$. Since $\mu = 1$ corresponds to forward projection of the protons, it is seen that the distribution at 50 Mev corresponds to a definite shift in the direction of forward-going protons. This may be understood as a consequence of the factor ζ^{-8} in the angular distribution which is

$$A_0(\mu) \sim (L/\zeta^4)^2 \sin^2\vartheta.$$

and is an expression of the fact that small recoil momenta are always strongly favored in any process arising from a slowly varying interac-

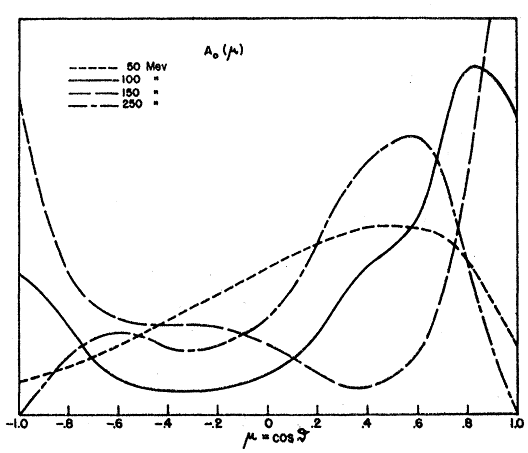

FIG. 2. The angular distribution of the photo-particles in the zero-momentum reference frame. The point $\vartheta = 0$ corresponds to protons in the direction of the incident photons. All curves normalized to the same area.

tion.[7] The finite number of particles at $\vartheta=0$ and π is due simply to the spin-transitions which contribute 28 percent to the total number of photo-disintegrations at this energy.

As the energy of the photon is increased to 100 and then to 150 Mev the tendency for forward ejection of the protons becomes more pronounced. This is understood at once by noting that at the higher energies the range of recoil momenta ($\zeta_{\max}/\zeta_{\min}$) is greater and the departure from the $\sin^2\vartheta$ distribution becomes so great that no resemblance to it remains. At the same time it is noted that a peak in the backward direction is developed. This is due to the increasing importance of the spin transitions in which both the proton and neutron play the role of a recoil particle. Superimposed on this distribution with peaks along and opposite to the direction of the photon are characteristic interference minima and maxima which are a reflection of the node in the L function (Fig. 1). This node tends to produce a minimum in the angular distribution at supplementary angles because of the relation between the directions of the recoil momenta of neutron and proton.

At 250 Mev the peaks in distribution are shifted from the extreme positions at $\vartheta=0$ and π and are therefore subdued in magnitude. This is an accidental effect of the destructive interference as may be seen by reference to Fig. 1, which shows that in this case the nodes of L occur near the ends of the angular range.

From the results given and from Fig. 1 it is possible to understand the feature of the angular distribution over the range from 50–250 Mev.

The angular distribution of the protons in the laboratory frame of reference is easily obtained from the foregoing. Designating the angle between the proton motion in the laboratory frame and the direction of propagation of the photon by $\vartheta_0=\arccos\mu_0$ and the distribution function by $A_L(\mu_0)$ we have

$$\mu_0=(\eta+\xi\mu)/(\xi^2+\eta^2+2\xi\eta\mu)^{\frac{1}{2}},$$

[7] At 50 Mev only about 10 percent of the wave-length of the photon is contained within the range of the nuclear forces. Even at 250 Mev the momentum of the photon is not very large. The strong effects of interference described below are mainly due to the fact that the wave-length of the particles, with energies in this range, is so much shorter than the range of the forces.

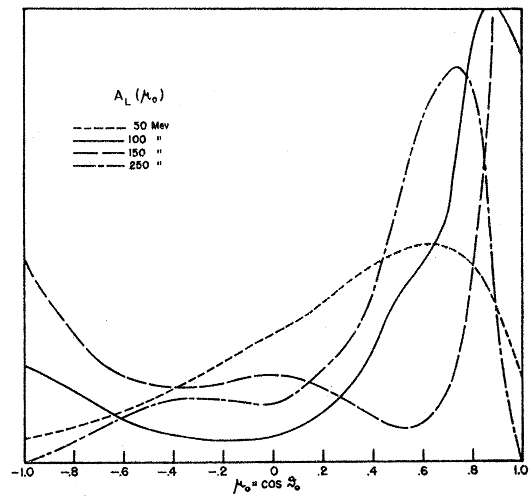

FIG. 3. The angular distribution of the protons in the laboratory frame of reference. The point $\vartheta=0$ corresponds to protons in the direction of the incident photon. All curves normalized to the same area. Ordinate scale same as in Fig. 2.

so that

$$A_L(\mu_0)=A_0(\mu)d\mu/d\mu_0$$
$$=A_0(\mu)(\xi^2+\eta^2+2\xi\eta\mu)^{\frac{3}{2}}/\xi^2(\xi+\eta\mu) \quad (15)$$

where

$$\xi=kR,\quad \eta=\tfrac{1}{2}k_0R. \quad (16)$$

The angular distribution of the protons $A_L(\mu_0)$ is shown in Fig. 3. Again for each γ-ray energy the normalization is the same and the scale in Figs. 2 and 3 is the same. The expected effect of the photon momentum in accentuating the forward peak is clearly evident.

(3) Energy Distribution

Because of the finite momentum of the photon the two nuclear particles do not share the available energy equally. In fact, the angular distribution $A_0(\mu)$ of Fig. 2 also represents the energy distribution of the particles. Designating the energies of proton and neutron, measured in the laboratory frame, by E_p and E_n, respectively, we have

$$E_p=\tfrac{1}{2}(\hbar\omega-\epsilon)+(EE_c)^{\frac{1}{2}}\mu,$$
$$E_n=\tfrac{1}{2}(\hbar\omega-\epsilon)-(EE_c)^{\frac{1}{2}}\mu,$$

where $E_c=(\hbar\omega)^2/4Mc^2$ is the center of gravity energy and $E=\hbar\omega-\epsilon-E_c$ is the kinetic energy of the relative motion in the zero-momentum reference frame. Therefore, Fig. 2 gives the

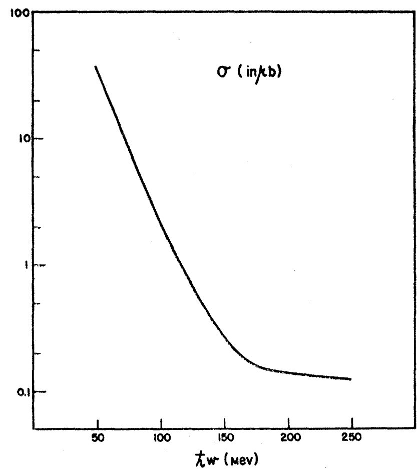

FIG. 4. Total cross section in μb (10^{-30} cm^2) on a logarithmic scale *versus* gamma-ray energy.

energy distribution of the protons (neutrons) if the linear μ-scale is replaced by a linear energy scale extending from the minimum energy $E_{\min}$ at the point $\mu=-1(+1)$ to the maximum energy $E_{\max}$ at $\mu=1(-1)$ and

$$\begin{pmatrix} E_{\max} \\ E_{\min} \end{pmatrix} = \tfrac{1}{2}(\hbar\omega-\epsilon)\pm(EE_c)^{\frac{1}{2}} = \tfrac{1}{2}(E^{\frac{1}{2}}\pm E_c^{\frac{1}{2}})^2.$$

Evidently the proton energy is on the average somewhat greater than the neutron energy because of the charge and the greater magnetic moment of the former.

(4) The Total Cross Section

The total cross section for photo-disintegration is obtained by numerical integration of the angular distribution. The results are shown in Fig. 4 in which the cross section is plotted on a logarithmic scale.

It may be noted first of all that the cross section is rather small in the energy range considered. This arises primarily from the destructive interference caused by the oscillations of the final state wave function inside the potential hole; for example, at 50 Mev, $\xi=kR=3.0$. At this energy the zero-range assumption gives a cross section of $130\mu b$ (μb = micro-barn = 10^{-30} cm^2) to be compared with the present value of $37.4\mu b$. This overestimate by a factor 3.5 is just about what is to be expected from a comparison of the zero range value of L (cf. Eq. (13a)).

$$L=\zeta^4/b^2(a^2+\zeta^2), \quad (R=0) \tag{13c}$$

with the correct value given by Fig. 1. As is to be expected, the situation is aggravated at 100 Mev where the effects of destructive interference are clearly evident. At this energy the cross section found here is $2.16\mu b$ whereas the zero range assumption gives a value about 30 times too large.

The second point to be noted is the rapid decrease in the cross section over the range 50–150 Mev. This is largely due to the fact that the cross section depends sensitively on the minimum recoil momentum which increases with $\hbar\omega$. Thus, the energy dependence of the contribution of the charge transitions is from (1), (9a), and (13)

$$\sigma_c \sim (k^3/\omega k k_0)(\zeta_{\min})^{-8}(L^2\sin^2\vartheta)_{\mathrm{Av}} \sim (L^2\sin^2\vartheta)_{\mathrm{Av}}/(\hbar\omega)^5,$$

since $\zeta_{\min}=(k-\frac{1}{2}k_0)R\sim kR$. The spin transitions give rise to a contribution σ_s which has an energy dependence given approximately by

$$\sigma_s/\sigma_c \sim k_0^2/k^2 \sim \hbar\omega/Mc^2.$$

Considering that the spin transitions become relatively more important with increase of $\hbar\omega$ and noting that $(L^2)_{\mathrm{Av}}$ decreases with $\hbar\omega$ near 50 Mev and then increases beyond 100 Mev, the energy dependence of the cross section in the region of the rapid decline may be understood. Beyond 150 Mev the cross section falls much more slowly because of the small role played by the destructive interference (see Fig. 1) and to the ever increasing importance of the contribution of the spin transitions.[8]

III. ADDITIONAL CONSIDERATIONS

In the following we present certain considerations bearing on the validity of the assumptions

[8] The small value of the cross section for the photo-effect at high energies explains the fact that the disintegration by high energy electrons is so much more effective than that by photons of the same energy. For example, the electron disintegration cross section at 100 Mev is 180 μb (Bethe and Peierls, reference 1) which is 80 times the cross section for 100-Mev photons. Clearly the electron disintegration is due almost entirely to the soft quanta arising from the contracted Coulomb field. Since the nuclear particles arising from the disintegration under electron bombardment are predominantly of low energy, the assumption of zero range of the nuclear forces should give the correct order of magnitude for the cross section in this case.

on which the foregoing calculations are based. These are (1) the neglect of nuclear forces in the final state and (2) the assumption of central forces in the ground state. In addition, calculations of the effect of retardation and higher multipoles are presented so that the conditions under which these effects can no longer be neglected may be more explicitly stated.

(1) Effect of Nuclear Forces in the Final State

Since the nuclear forces are most effective at the lower γ-ray energies, we consider only those transitions induced by the coupling between the electric dipole part of the radiation and the proton charge. While the neglect of the spin transitions even at 50 Mev is not justifiable, both types of transitions depend on the same matrix element and therefore an estimate of the effect under consideration may be obtained from the consideration of the charge transitions only. The effect of retardation is retained.

With central forces only the final state is ${}^3P$, so that

$$\psi_f = 3ie^{-i\delta}F(kr)\cos\Theta,$$

where δ is the phase shift of the radial function $F(kr)$ and Θ is the angle between $\mathbf{k}$ and $\mathbf{r}$. We represent the P state interaction by a rectangular well of depth V_P and range R. Introducing the notation

$$f_n(y) = (\pi/2y)^{\frac{1}{2}}J_{n+\frac{1}{2}}(y),$$

$$g_n(y) = -(\pi/2y)^{\frac{1}{2}}J_{-n-\frac{1}{2}}(y)$$

where the J's are Bessel functions, we have

$$F = (\cos\delta f_1(\xi)+\sin\delta g_1(\xi))f_1(\xi_P x)/f_1(\xi_P), \quad x<1 \quad (17a)$$

$$F = \cos\delta f_1(\xi x)+\sin\delta g_1(\xi x), \quad x>1 \quad (17b)$$

where we have used the notation introduced in (11) and (16) and

$$\xi_P = R[M(E-V_P)]^{\frac{1}{2}}/\hbar. \quad (16a)$$

The phase shift is given by

$$\cot\delta = -\frac{\xi_P g_1(\xi)f_0(\xi_P)+\xi g_0(\xi)f_1(\xi_P)}{\xi_P f_1(\xi)f_0(\xi_P)-\xi g_0(\xi)f_1(\xi_P)}. \quad (18)$$

From (7a) we obtain

$$W_c = -(24\pi R/k_0)e^{-i\delta}\sin\vartheta\sin\varphi\,\delta_{m_s m_s'} \times\int_0^\infty F(\xi x)f_1(\eta x)(d\psi_i/dx)xdx, \quad (19)$$

where ϑ and φ represent the angle between $\mathbf{k}_0$ and $\mathbf{k}$ and the azimuth of the polarization vector $\boldsymbol{\pi}$, respectively. Then

$$(|W_c|^2)_{\text{Av}} = (36\pi R/\eta^2) \times\sin^2\vartheta(a^3b/1+a)(Y_i+Y_0)^2, \quad (20)$$

$$Y_i = -\frac{b}{a}\,\frac{\cos\delta f_1(\xi)+\sin\delta g_1(\xi)}{f_1(\xi_P)} \times\int_0^1 f_1(\xi_P x)f_1(\eta x)f_1(bx)xdx, \quad (20a)$$

$$Y_0 = \frac{\sin b}{b}e^a\int_1^\infty [\cos\delta f_1(\xi x)+\sin\delta g_1(\xi x)] \times f_1(\eta x)e^{-ax}(1+1/ax)dx. \quad (20b)$$

The integrals in Y_i and Y_0 were computed numerically for a series of values of the depth of the P well ranging from 15 Mev attractive to 10 Mev repulsive.[9] The cross section σ_c increases approximately linearly by about $1\mu b$ per Mev repulsion (see Table I). Therefore, the effect of nuclear forces may be expected to change the cross section at 50 Mev by 30 percent or less. At higher energies the correction will, of course, be smaller.

(2) Effect of Retardation and Higher Multipoles

Again restricting our attention to the electric dipole transition, the effect of neglecting retarda-

TABLE I. Cross sections in μb for charge transitions.

Multipoles	V_P(Mev)	Retardation	σ_c(50 Mev)	σ_c(100 Mev)
all	0	with	27.8	0.89
el. dipole	0	with	27.4	
el. dipole	0	without	27.6	0.46
el. dipole	15	with	10.3	
el. dipole	15	without	10.1	
el. dipole	−10	without	39.2	

[9] While no reliable data exist from which the P interaction can be deduced it is of interest to note that the proton-proton scattering at 10 Mev indicates an interaction which certainly falls within the range cited above. See R. R. Wilson, Phys. Rev. **71**, 384 (1947).

tion is obtained by replacing $f_1(\eta x)$ in (20a) and (20b) by its value for small argument,[10]

$$f_1(\eta x)\sim\tfrac{1}{3}\eta x.$$

The integrals can then be carried out analytically and we find

$$Y_i=\frac{\eta b}{3a}\frac{\cos\delta f_1(\xi)+\sin\delta q_1(\xi)}{f_1(\xi_P)}\times\frac{bf_1(\xi_P)f_0(b)-\xi_P f_1(b)f_0(\xi_P)}{\xi_P{}^2-b^2},\qquad(21\text{a})$$

$$Y_0=\frac{\eta}{3}\frac{\sin b}{b}\frac{1}{\xi^2+a^2}\{\cos\delta[af_1(\xi)+\xi f_0(\xi)(1+1/a)]+\sin\delta[ag_1(\xi)-\xi g_0(\xi)(1+1/a)]\}.\qquad(21\text{b})$$

The numerical results for the electric dipole cross section are compared with the corresponding results with retardation and with the cross section due to all multipoles in Table I. The The first two rows of the table show that the effect of higher multipoles is negligible at 50 Mev. The comparison between the second and third as well as between the fourth and fifth rows shows that the effect of retardation is negligible at 50 Mev. On the other hand, from rows one and three it is seen that at 100 Mev the effect of retardation and higher multipoles is important.

(3) Effect of Tensor Forces

The effect of non-central forces in the ground state of the deuteron may be estimated using the model of Rarita and Schwinger.[11] The initial state wave function now becomes

$$\Psi_i=\Phi_{01m}U_S+\Phi_{21m}U_D,\qquad(22)$$

where Φ_{LJm} are normalized spin angular functions[11] corresponding to orbital and total angular momentum $L\hbar$ and $J\hbar$, respectively, while $J_z=m$. The radial wave functions for the S and D parts of the ground state are U_S and U_D, respectively. The final state wave function is given by (6) and (6a).

A straightforward calculation gives for the charge transitions

$$(|W_c|^2)_{\text{Av}}=2\pi k^2\sin^2\vartheta(B_S{}^2+B_D{}^2),\qquad(23)$$

where

$$B_S=\int_0^\infty U_Sf_0(qr)r^2dr,$$

$$B_D=\int_0^\infty U_Df_2(qr)r^2dr.$$

In the absence of tensor coupling $B_D=0$ and $B_S=B_S{}^{(0)}$ where

$$B_S{}^{(0)}=\int_0^\infty U_S{}^{(0)}f_0(qr)r^2dr.$$

The radial wave functions are normalized as follows:

$$\int_0^\infty r^2(U_S{}^{(0)})^2dr=1,\qquad\int_0^\infty r^2(U_S{}^2+U_D{}^2)dr=1.$$

To a good degree of approximation we can set[11]

$$U_S=\nu_1U_S{}^{(0)},$$

where ν_1 is a constant. From the normalization conditions we get[11]

$$\nu_1{}^2=1-\int_0^\infty U_D{}^2r^2dr=0.96.$$

Therefore we obtain a lower limit for the charge cross section

$$\sigma_c>\nu_1{}^2\sigma_c{}^{(0)}=0.96\sigma_c{}^{(0)},\qquad(24)$$

where again the superscript zero refers to central forces.

The term $B_D{}^2$ which represents the difference between the two sides of the inequality (24) is a small term. In this term we are therefore justified in making the somewhat rougher approximation

$$U_D=\nu_2U_S,$$

where ν_2 is a constant. This is justified over a

[10] As a check on our results we may reduce the cross section to the Bethe-Peierls result (reference 1) which is readily obtained as the limiting case for zero range and zero P well. Thus, in the limit $Y_i=0$ and $Y_0=(\eta\xi/3a)\times(\sin b/b)(\xi^2+a^2)^{-1}$. With $b=\pi/2$ the cross section becomes (from (1) and (20))

$$\sigma_c=\frac{8\pi}{3}\frac{e^2}{\hbar c}\frac{\hbar^2}{M}\frac{E^{\frac{1}{2}}\epsilon^{\frac{3}{2}}}{(E+\epsilon)^3}.$$

In the limit $R=0$ the result of II, Section 4 reduces to the cross section given by Jauch (reference 3).

[11] W. Rarita and J. Schwinger, Phys. Rev. **59**, 436 (1941).

region $0.5 < r/R < 1.5$ from which the integral B_D gets its main contribution. From the normalization we get

$$(1+\nu_2^2)\nu_1^2 = 1.$$

For small argument qr the function $f_0 \gg f_2$ but for arguments of order π or greater the two functions are of about equal magnitude and differ in sign. Therefore, we replace f_2 by f_0. If anything, this should overestimate B_D. Then

$$B_S^2 + B_D^2 \lesssim \nu_1^2(1+\nu_2^2)(B_S^{(0)})^2 = (B_S^{(0)})^2 \quad (25)$$

or

$$\sigma_c \lesssim \sigma_c^{(0)}.$$

From (24) and (25) we may conclude that the effect of tensor forces on the charge cross section, and therefore on the total cross section, is 4 percent or less.